



HHS Public Access

Author manuscript

Nat Biomed Eng. Author manuscript; available in PMC 2020 January 22.

Published in final edited form as:

Nat Biomed Eng. 2019 October ; 3(10): 806–816. doi:10.1038/s41551-019-0431-2.

immune-orthogonal orthologues of AAV capsids and of Cas9 circumvent the immune response to the administration of gene therapy

Ana M. Moreno^{a,*}, Nathan Palmer^{b,*}, Fernando Alemán^c, Genghao Chen^a, Andrew Pla^a, Ning Jiang^d, Wei Leong Chew^e, Mansun Law^c, Prashant Mali^{a,†}

^aDepartment of Bioengineering, University of California San Diego, CA, USA.

^bDivision of Biological Sciences, University of California San Diego, CA, USA.

^cDepartment of Immunology and Microbiology, The Scripps Research Institute, CA, USA.

^dDepartment of Biomedical Engineering, The University of Texas at Austin, TX, USA.

^eSynthetic Biology, Genome Institute of Singapore, Singapore.

Abstract

Protein-based therapeutics can activate the adaptive immune system and lead to the production of neutralizing antibodies and to cytotoxic-T-cell-mediated clearance of the treated cells. Here, we show that the sequential use of immune-orthogonal orthologues of the CRISPR-associated protein 9 (Cas9) and of adeno-associated viruses (AAVs) eludes adaptive immune responses and enables effective gene editing from repeated dosing. We compared total sequence similarities and predicted binding strengths to class-I and class-II major-histocompatibility-complex proteins for 284 DNA-targeting and 84 RNA-targeting CRISPR effectors, and for 167 AAV VP1-capsid-protein orthologues. We predict the absence of cross-reactive immune responses for 79% of the DNA-targeting Cas orthologs, which we validate for three Cas9 orthologs in mice, yet anticipate broad immune cross-reactivity among the AAV serotypes. We also show that efficacious *in vivo*

Users may view, print, copy, and download text and data-mine the content in such documents, for the purposes of academic research, subject always to the full Conditions of use:http://www.nature.com/authors/editorial_policies/license.html#terms

[†]Correspondence: pmali@ucsd.edu.

*These authors contributed equally.

AUTHOR CONTRIBUTIONS

A.M. designed and performed experiments, analyzed the data, and wrote the manuscript. N.P. performed the *in silico* analysis, designed and performed experiments, analyzed the data, and wrote the manuscript. F.A. performed the ELISPOT experiments and analyzed the data. G.C. and A.P. helped perform experiments. N.J., W.L.C., and M.L. helped design experiments. P.M. supervised the project, designed and helped perform experiments, and wrote the manuscript.

COMPETING INTERESTS

A.M., N.P., and P.M. have filed patents based on this work. P.M. is a scientific co-founder of Navega Therapeutics, Pretzel Therapeutics, Seven Therapeutics, Engine Biosciences, and Shape Therapeutics. The terms of these arrangements have been reviewed and approved by the University of California, San Diego in accordance with its conflict of interest policies.

DATA AVAILABILITY

The authors declare that the main data supporting the results in this study are available within the paper and its Supplementary Information. The raw and analysed datasets generated during the study are available for research purposes from the corresponding authors on reasonable request.

CODE AVAILABILITY

All code, input and output files used in this study are publicly available on GitHub (<https://github.com/natepalmer/immune-orthogonal>). Additional modified scripts can be accessed upon request.

gene editing is uncompromised when using multiple dosing with orthologues of AAVs and Cas9 in mice previously immunized against the AAV vector and the Cas9 payload. Multiple dosing with protein orthologues may allow for sequential regimens of protein therapeutics that circumvent pre-existing immunity or induced immunity.

Protein therapeutics, including protein-based gene therapy, have several advantages over small-molecule drugs. They generally serve complex, specific functions, and have minimal off-target interference with normal biological processes. However, one of the fundamental challenges to any protein-based therapeutic is the interaction with the adaptive immune system. Neutralization by circulating antibodies through B-cell activation and clearance of treated cells by CD8+ cytotoxic T-lymphocytes (CTLs) create a substantial barrier to effective protein therapies¹⁻⁴. Although for some applications the delay in the adaptive immune response to novel proteins may allow sufficient time for the initial dose to work, subsequent doses face faster and stronger secondary immune responses due to the presence of memory T- and B- cells. In addition, gene transfer studies have shown that host immune responses against the delivery vector and/or therapeutic transgene can eliminate treated cells, thus limiting the efficacy of the treatment⁵⁻¹¹.

A common approach to circumventing these issues has been to utilize human proteins, or to humanize proteins by substitution of non-human components^{12,13}. However, this approach is limited to a small set of therapeutic proteins naturally occurring in humans or closely related species. In addition, although the humanization of proteins can result in a significantly less immunogenic product, they still carry immunological risk¹³. Another way to circumvent an immune response to protein therapeutics is the removal of immunogenic T cell epitopes¹⁴⁻¹⁶. Once these epitopes are identified, substitution of key amino acids may reduce the protein's immunogenicity since modification of critical anchor residues can abrogate binding to MHC (Major Histocompatibility Complex) molecules and prevent antigen presentation. However, this can prove difficult due to the massive diversity at HLA (Human Leukocyte Antigen) loci. As epitope engineering must account for the substrate specificity of each different HLA allele, therapeutics would likely require unique modification for each patient. While epitope deletion/mutation has been successfully applied to several proteins^{16,17}, this can only preserve protein function when limited to small numbers of HLA alleles unrepresentative of the full diversity. Structural modifications such as PEGylation have also been known to reduce immunogenicity by interfering with antigen-processing mechanisms. However, there is evidence that PEG(PolyEthylene Glycol)-specific antibodies are elicited in patients treated with PEGylated therapeutic enzymes¹⁸⁻²¹.

Furthermore, protein therapies often require repeated treatments due to degradation of the protein, turnover of treated cells, or, in the case of gene therapy, reduced expression of the transgene^{22,23}. This provides an even greater challenge as repeated exposure to the same antigen can elicit a more robust secondary immune response²⁴, which may completely inhibit subsequent dosage or even sensitize the immune system to antigens remaining from the initial exposure. In order to facilitate efficacious repeat protein therapies, we propose the use of orthologous proteins whose function is constrained by natural selection, but whose structure is subject to diversification by forces such as genetic drift. An ortholog, given

sufficient sequence divergence, will not cross-react with the immune response generated by exposure to the others, allowing repeat doses to avoid neutralization by existing antibodies and treated cells to avoid clearance by activated CTLs.

As a case study for exploring this approach we focused on the CRISPR (Clustered Regularly Interspaced Short Palindromic Repeats)-Cas9 system, perhaps the most anticipated therapeutic for gene editing²⁵⁻³⁵. Comparative genomics has demonstrated that Cas9 proteins are widely distributed across bacterial species and have diversified over an extensive evolutionary history³⁶⁻⁴⁰. Although there may be pre-existing immunity to Cas9s from pathogenic or commensal species⁴¹⁻⁴³, we hypothesized this diversity could provide a mechanism to circumvent inducing immunological memory by utilizing orthologous Cas9 proteins for each treatment.

An additional important consideration is the immunogenicity of the delivery vehicle or administration route for the Cas9 and associated guide RNA (gRNA). In this regard, adeno-associated viruses (AAVs) have emerged as a highly preferred vehicle for gene delivery, as they are associated with low immunogenicity and toxicity^{8,9}, which promotes transgene expression^{44,45} and treatment efficacy. Despite the relatively low immunogenicity of AAV vectors, antibodies against both the capsid and transgene may still be elicited^{10,46-52}. Additionally, the prevalence of neutralizing antibodies (NAB) against AAVs in the human population⁵³ and cross-reactivity between serotypes⁵⁴ remains a hurdle for efficacious AAV therapy. Although AAVs were initially considered non-immunogenic due to their poor transduction of antigen-presenting cells (APCs)⁵⁵, it is now known that they can transduce dendritic cells (DCs)⁵⁶ and trigger innate immune responses through Toll-like receptor (TLR) signaling pathways⁵⁷. The ability to transduce DCs is dependent on AAV serotype and genome, and may be predictive of overall immunogenicity⁵⁸. A previous study exploring the utility of the AAV-Cas9 system observed a humoral immune response to both AAV and Cas9, as well as an expansion of myeloid and T-cells in response to Cas9⁵², highlighting the need to confront this issue when further developing gene therapies.

To evaluate the immune orthogonality of AAV-delivered CRISPR-Cas systems, we analyzed 284 DNA targeting and 84 RNA targeting CRISPR effectors, and 167 AAV VP1 orthologs. By comparing total sequence similarity as well as predicted binding strengths to class I and class II MHC molecules, we constructed graphs of immune cross-reactivity and computed cliques of proteins that are orthogonal in immunogenicity profiles. Although MHC epitopes do not predict antibody epitopes, the induction of the more powerful memory response is primarily dependent on reactivation of memory B-cells with help from memory T-cells through the presentation of antigens on class II MHC molecules^{59,60}. Next, we experimentally confirmed our immunological predictions by assaying treated mice for induction of protein-targeting antibodies and of T-cell-mediated cytotoxicity against AAV and Cas9 proteins. Finally, we demonstrated in multiple contexts that consecutive dosing with immune-orthogonal orthologs circumvents the inhibition of effective gene editing caused by immune recognition of the AAV vector and Cas9 transgene.

RESULTS

Immune response to AAV and Cas9

One of the major obstacles for sequential gene therapy treatments is the presence of neutralizing antibodies against the delivery vehicle and transgene cargo induced by the first administration of the therapy (Figure 1A). To determine the humoral immune response kinetics to AAV-CRISPR therapeutics (Figure 1B), focusing as an exemplar on the AAV8 capsid and the Cas9 transgene, we first injected C57BL/6J mice retro-orbitally with 10^{12} vg of AAV8-SaCas9 targeting proprotein convertase subtilisin/kexin type 9 (PCSK9), a promising gene target that when disrupted can reduce Low Density Lipoprotein (LDL) levels and protect against cardiovascular disease. Consistent with a previous study⁶¹, mice had reduced PCSK9 serum levels as early as one week post-injection due to successful SaCas9 mediated gene-editing, which was sustained for the entire duration of the experiment (4 weeks) (Figure 1C). We noted that a subset of the mice developed IgG1 antibodies against the SaCas9 protein (Figure 1D). Additionally, mice developed humoral immunity to the AAV8 capsid within one-week post-injection (Figure 1E). Finally, we also confirmed a CD4+ T-cell response against AAV8 and SaCas9 for a subset of predicted MHCII epitopes on these proteins using an ELISPOT (Enzyme-Linked Immunospot) (Figure S1). To evaluate the feasibility of multiple dosing with AAV-Cas9, we next investigated whether immune orthogonal sets of AAV and Cas9 orthologs exist.

Identifying immune-orthogonal proteins

Natural selection produces diverse structural variants with conserved function in the form of orthologous genes. We assayed the relevance of this diversity for immunological cross-reactivity of 284 DNA targeting and 84 RNA targeting CRISPR effectors (Table S1) and 167 AAV orthologs (Table S2) by first comparing their overall amino acid sequence similarities, and second, using a more specific constraint of how their respective amino acid sequences are predicted to bind MHC Type I and II molecules (Figure 1F). From these analyses we obtained first an estimate of the comprehensive immune overlap among Cas and AAV orthologs based purely at the sequence level, and second a more stringent estimate of predicted immune overlap based on predicted MHC binding (Figures 1G, 1H, S2). By sequence-level clustering and clique finding methods, we defined many sets of Cas9 orthologs containing up to 9 members with no 6-mer overlap (Figure S3). Notably, based on MHC-binding predictions, we find among the set of DNA-targeting Cas proteins (240 Cas9s and 44 Cpf1s) that 79% of pairs are predicted to have non cross-reacting immune responses, i.e. they are predicted to be orthogonal in immune space (Figure 1G). On the contrary, among AAV capsid (VP1 protein) orthologs we did not find full orthogonality up to the 14-mer level, even when restricting predictions with MHC-binding strengths (Figure 1H), likely reflecting the strong sequence conservation and shorter evolutionary history of AAVs⁶². This analysis suggests, consistent with previous observations^{63,64}, that exposure to one AAV serotype can induce broad immunity to all AAVs, which presents a significant challenge to AAV delivery methods, as some serotypes are prevalent in human populations. Despite the most divergent AAV serotype (AAV5) showing the fewest shared immunogenic peptides, there remain tracts of sequences fully conserved within the VP1 orthologs. As expected, predicted immune cross-reaction negatively correlates with phylogenetic distance (Figure

S4), though there is significant variation not captured by that regression, suggesting that MHC-binding predictions can refine the choice of sequential orthologs beyond phylogenetic distance alone.

Confirming humoral immune-orthogonality among Cas9 proteins

To test our immunological predictions and to establish the utility of this approach, we narrowed in on a 5-member clique containing the ubiquitously used *S. pyogenes* Cas9 in addition to the well-characterized *S. aureus* Cas9 (Figure S3). To determine whether either of these proteins have cross-reacting antibody responses, we injected mice with 10^{12} vg of either AAV8 or AAVDJ capsids containing SaCas9 or SpCas9 transgenes via retro-orbital injections and harvested serum at days 0 (pre-injection), and periodically over 4–6 weeks (Figure 2A). SpCas9-specific antibodies were detected in the plasma of all mice injected with SpCas9 (n=6), and notably none of the mice injected with SaCas9 (n=12) (Figure 2B). Half of the mice injected with SaCas9 AAVs (n=12) developed detectable antibodies against SaCas9, whereas none of the mice injected with SpCas9 AAVs (n=6) developed an antibody response against SaCas9. These results were confirmed in an independent study in which SpCas9-specific antibodies, but not SaCas9-specific antibodies, were detected in the plasma of mice injected with AAV-SpCas9 (n=12). These mice were injected retro-orbitally with 10^{12} vg of AAV8-SpCas9 or AAVDJ-SpCas9, and also received an additional intramuscular injection with 10^{11} vg at week 4. (Figure 2C). Taken together, our data confirms that SpCas9 and SaCas9 have humoral immune-orthogonality. As an additional step, we tested another Cas9 ortholog from *Campylobacter jejuni*, useful for AAV-based delivery due to its small size. Mice injected retro-orbitally with 10^{12} vg AAV8-CjCas9 (n=12) showed no significant humoral response to Sp- or SaCas9 after 4 weeks (Figure S5), confirming immune orthogonality for a set of 3 unique Cas9 orthologs.

Confirming broad immune cross-reactivity among AAV serotypes

AAVs are becoming a preferred delivery vehicle due to their ability to avoid induction of a strong CD8+ T-cell response, however, the presence of neutralizing antibodies remains a significant barrier to successful application of AAV therapies. Consistent with previous results⁶³, we found shared immunogenic peptides among all human AAV serotypes (Figure S6). We confirmed the lack of orthogonality for two serotypes, AAV8 and AAVDJ, in which we found that antibodies produced in mice injected with AAV8 or AAVDJ react to both AAV8 and AAVDJ antigens (Figure 2D). Our analysis suggests that there are no two known AAVs for which exposure to one would guarantee immune naïveté to another across all MHC genotypes. However, immune cross-reaction could be minimized through the use of AAV5^{64,65}, the most phylogenetically divergent serotype. Our predictions identify only a single shared highly immunogenic peptide between AAV5 and the commonly used AAV2 and AAV8 in the mouse model (though several other shared peptides of mild MHC affinity exist). We confirmed this via ELISAs (enzyme-linked immunosorbent assay), where mice injected with AAV2 did not elicit antibodies against AAV5 and AAV8, and mice injected with AAV5 did not elicit antibodies against AAVDJ and AAV8 (Figure 2D).

Overcoming immune barriers to effective gene editing

Having demonstrated that AAV-Cas9s elicit an immune response in the mouse model, and that the humoral responses to SpCas9 and SaCas9 do not cross-react, we next performed a two-step dosing experiment to test whether these immune responses inhibit the efficacy of multi-dose gene editing, and whether using immune-orthogonal orthologs in sequence can avoid immune-mediated inhibition of gene editing (Figures 3A, S7). For this experiment, we used another mouse strain, BALB/c, in order to verify and characterize the immune response in two independent strains. The first round of dosing contained no gRNA and served to immunize the mice against the second dose, which contained an active AAV8-SaCas9 with gRNA targeting PCSK9, allowing us to directly measure genome editing efficiency by sequencing, as well as serum PCSK9 levels as a phenotypic readout for therapeutic efficacy. Additionally, we measured IgG responses to all AAV and Cas9 used in the experiment. As expected from previous preclinical work on AAV therapies, prior exposure and humoral immunity to AAV8 (AAV8-mCherry) abolished the effectiveness of subsequent gene editing when using AAV8 as the delivery vector (AAV8-SaCas9). Importantly, this effect was not seen with previous exposure to AAV5 (AAV5-mCherry), and subsequent dosing with AAV8-SaCas9 resulted in strong genome editing and PCSK9 knockdown similar to the effects of AAV8-SaCas9 dosing in naïve mice (Figures 3B, 3C).

Although we do not necessarily expect this observed orthogonality between AAV8 and AAV5 to carry over into the human setting, here it allowed us to specifically test the effects of the immune response to the Cas9 payload with minimal interference from the AAV delivery vector. Mice first immunized against SaCas9 using AAV5 showed a 35% reduced level of editing, a 38% reduction in PCSK9 decrease, and a wider variation between mice. This may reflect a weak immune response to SaCas9 in our mouse model, and/or a domination of private (individual) T-cell responses to SaCas9. IgG ELISAs revealed that only a subset of mice immunized with AAV5-SaCas9 developed an antibody response. We correlated the level of serum antibodies induced upon SaCas9 immunization with the efficiency of PCSK9 editing after the second dose, finding that mice with a stronger antibody response showed lower editing efficiency (Figure 3D). In contrast, we found that mice first dosed with AAV5-SpCas9 showed robust editing similar to that in naïve mice, suggesting that the predicted and measured immune orthogonality of Sp- and SaCas9 can be harnessed to circumvent immune barriers to gene editing.

To replicate these results in a different context, and to verify that immunity to Cas9 specifically can create a barrier to effective gene therapy, we conducted a slightly modified immunization experiment. Here we used a Cas9 protein vaccine combined in emulsion with Complete Freund's Adjuvant (CFA) as the initial dose, thereby immunizing a Cas9-specific primary response independently of AAV (Figure 3D). Subsequent dosing with AAV8-SaCas9 targeting PCSK9 recapitulated the results of AAV-based immunization, showing that prior exposure to the SaCas9 protein, but not SpCas9, significantly reduced the effectiveness of SaCas9-based gene editing (Figure 3E, 3F). Additionally, we also tested the ability of CFA-Cas9 immunized mice to clear injected splenocytes pulsed with immunogenic Cas9 epitopes. We observed specific clearance of Cas9-pulsed cells 3.5 weeks after immunization,

demonstrating that anti-Cas9 T-cells can specifically recognize and kill cells presenting Cas9 epitopes (Figure S8).

Taken together, anti-AAV and anti-Cas9 immunity represents a significant obstacle to therapeutic efficacy, and the use of immune orthogonal AAVs and Cas proteins, by bypassing immune recall, enables effective gene-editing from repeated administrations of these therapeutic modalities.

DISCUSSION

The use of protein therapeutics requires ways to evade the host's immune response. Cas9, as an example, has prokaryotic origins and can evoke a long-lived T-cell response^{42,52}, which may lead to clearance of transduced cells. In addition, circulating antibodies can neutralize the AAV vector and prevent efficient transduction upon repeated doses. Immunosuppressive drugs could mitigate some of these aspects, but not without significant side-effects, and are not applicable to patients in poor health⁶⁶⁻⁶⁹. Similar to what has been done in cancer antibody therapeutics⁷⁰, the SpCas9 protein could be de-immunized by swapping high-immunogenicity domains. This is a promising approach; however, it will be complex and laborious as we anticipate tens of mutations to achieve stealth, which might often result in a reduction in activity and an overall less effective therapy.

Another consideration is that various applications of the CRISPR system will have significantly different immune consequences. For example, contrast genome editing applications, in which only transient expression of Cas9 is needed, to cases of gene regulation (CRISPRi or CRISPRa), in which continuous Cas9 expression is required. While ongoing expression applications will have to continuously contend with T-cell surveillance, genome editing with transient expression may not be compromised by a primary T-cell response if Cas9 expression is lost before CTL activation and clonal expansion. Building on this advantage, we note that promising new techniques may achieve stable gene regulation via transient i.e. hit-and-run approaches using epigenome editing⁷¹. Despite this, efficacious single-dose therapies may require high titers, especially in cases such as Duchenne muscular dystrophy where systemic delivery is needed. Such high doses may lead to toxicity issues, as demonstrated in a recent study of high-dose AAV9 delivery in rhesus macaques⁷². Multiple lower, non-toxic doses delivered sequentially have the potential to achieve high transduction efficiency but must contend with the stronger and faster secondary adaptive immune response mediated by memory T- and B-cells.

To circumvent this issue, we developed here a framework to compare protein orthologs and their predicted binding to MHC I and MHC II by checking a sliding window of all k-mers in a protein for their presence in another, focusing on peptides predicted to bind to at least one MHC allele. Through this analysis, we identified cliques of Cas9 proteins that are immune orthogonal. Based on these predictions, specific T-cell responses from one ortholog would not cross-react with another ortholog of the same clique, preventing the re-activation of CD8+ cytotoxic T-cells, as well as the CD4+ T-cell help necessary to re-activate memory B-cells. We confirmed these results through ELISAs and verified three well-characterized Cas9 proteins (SpCas9, SaCas9, and CjCas9) to be immune orthogonal. Finally, we demonstrated

in multiple contexts that consecutive dosing with the same AAV or Cas9 ortholog can face diminished editing efficacy which can be overcome with the use of immune orthogonal orthologs. Therefore, we expect that proteins belonging to the same clique can be used sequentially without eliciting memory T- and B- cell responses.

An important caveat is that each sequential ortholog should also be immune orthogonal to the pre-existing immune repertoire. Very recent work has begun to explore pre-existing immunity to Sp- and SaCas9^{41–43} in human donors. One potential repository of Cas9 to which humans may not have any pre-existing immunity is in the genomes of extremophiles. However, although humans are not likely to be exposed to these organisms previously, their Cas9s may nevertheless be closely related to commensal or pathogenic species, and therefore immune orthogonality to pre-existing immunity must be rigorously evaluated. To explore this issue, we categorized 240 Cas9s orthologs based on their species of origin as commensal, pathogenic, environmental, or extremophile, and compared the immune orthogonality between these groups (Figure S9). Preliminary analysis suggests that there may be extremophile Cas9s divergent enough as to be orthogonal to pre-existing immunity, even when taking into account both pathogens and commensals. Many more candidates are likely to be discovered as we continue cataloging microbial diversity in a variety of environments using metagenomic approaches. Alongside this process, more diverse Cas9s must be tested and studied to determine if and under what conditions they will be usable in a mammalian setting.

Due to the importance of AAVs as a delivery agent in gene therapy, we also analyzed AAV serotypes through our MHC I and II comparison framework and have demonstrated that no two AAVs are predicted to be entirely immune orthogonal. However, with a known HLA genotype, it may be possible to define a personalized regimen of immune orthogonal AAVs using currently defined serotypes. For instance, use of AAV5 minimizes immune cross-reactivity in mice and non-human primates, as demonstrated by a recent study in which chimeric-AAV5 immunized mice and non-human primates successfully received a second dose of treatment with AAV1⁶⁵. However, in the human setting we predict that there may be substantially more immune overlap between AAV5 and other AAVs. Additionally, it has been shown that memory B-cells heavily contribute to the antibody response to similar but not identical antigens⁷³, indicating that partial orthogonality may not be sufficient. Our analysis suggests that creating a pair of globally orthogonal AAV capsids for human application would require >10 mutations in one of the two proteins. This hypothetical orthogonal AAV capsid presents a substantial engineering challenge, as it requires mutating many of the most conserved regions to achieve immune orthogonality.

Although we characterize the adaptive immune response to both the AAV VP1 and Cas9 proteins, it is not expected that these will induce the same type nor kinetics of response due to the differing nature of the antigens. The mice receive VP1 protein in the form of a viral capsid, as contrasted with Cas9 in the form of DNA. The delivery of AAV capsids is expected to produce a strong antibody response through the canonical MHC class II pathway. It may also induce a CTL response through MHC class I presentation via transduction of APCs or cross-presentation of endocytosed viral proteins.

Alternatively, the Cas9 transgene is expressed as protein only once inside a transduced cell, and therefore could be expected to induce both an antibody and CTL response through two separate but non-mutually exclusive mechanisms. One potential avenue is that a subset of AAVs transduce APCs, an event that has been previously observed to occur⁵⁶. After expression, Cas9 may be presented on class I MHC molecules through the canonical pathway, or presented on class II MHC molecules after being encapsulated in autophagosomes (a substantial fraction of MHCII-bound peptides is derived from internal proteins through autophagy)⁷⁴. Another potential mechanism involves transduced non-APCs expressing Cas9 and subsequently undergoing apoptosis or necrosis. APCs then scavenge these dying cells, presenting the Cas9 proteins found within on class II MHC molecules through the canonical pathway, or on class I MHC molecules through cross-presentation, a process important for anti-viral immune responses.

Previous work has identified that MHC affinity is highly dependent on anchor residues at either end of the binding pocket⁷⁵. Residue diversity is more tolerated in the center of the binding pocket, though it may be these residues that most impact antigen specificity, as it is thought that they are central to interaction with the T-cell receptor (TCR). Comparing the number of orthologous pairs in 9-mer space with the number of predicted orthologous pairs based on class II binding predictions suggests that only approximately 65% of 9-mer peptides serve as appropriate MHC class II binding cores, even across the thousands of HLA-2 combinations we explore here. This under-sampling of peptide space by MHC molecules likely reflects the requirement for hydrophobic anchor residues and leaves some space for protein de-immunization by mutation of immunogenic peptides to ones which never serve as MHC binding cores. Achieving this while preserving protein function however, has proven difficult even for few HLA alleles, and remains a major protein engineering challenge. New technologies for directly measuring TCR affinity with MHC-presented antigens⁷⁶ will also further clarify the key antigenic peptides contributing to the immune response, and will be useful to inform approaches here.

We also note some limitations to our work. Mainly, we have used two inbred mice strains, C57BL/6J and BALB/c, as our model, which have limited MHC diversity⁷⁷, and might not recapitulate other human immunological features, such as differences in antigen processing and presentation. Our use of highly conservative models of potential human immunity suggests that any immune barriers to gene editing we observe here could be significantly magnified in the human setting. In this regard, we attempted to measure the human T-cell response with the IFN- γ ELISPOT assay for a subset of predicted MHCI and MHC II peptides (**refer** Tables S3, S4), corroborating recent studies of pre-existing immunity to Sp- and SaCas9 in humans^{16,41,42} that showed measurable effector and regulatory T-cell responses. In our C57BL/6J model, we observed a low CD4+ T-cell response against specific MHCII peptides with mice injected with SaCas9 (Figure S1). One promising approach is to harness the ability of Treg cells to promote a more tolerogenic immune response to therapeutic proteins⁴². Additionally, B-cell epitopes can also be predicted and incorporated into immune orthogonality analysis. However, since B-cell epitopes may be both linear and conformational, these are more difficult to predict. Advances and further validation of these *in silico* models will allow for better predictions in the future^{78–82}. In our

study, initial immunization doses were not delivered with a gRNA, therefore Cas9 produced inside the cell or delivered as a protein will be in the apo-Cas9 conformation. This could result in different B-cell epitopes compared to the gRNA-bound Cas9 complex, as the 3D conformations are substantially different. Note that this should not affect MHC-presented peptides however, and thus not affect T-cell responses. Finally, recent work has indicated that MHC class I peptides may have significant contribution from spliced host and pathogen-derived peptides created by proteasomal processing⁸³. It is unclear how this may affect cross-recognition of proteins we predict to be immune orthogonal. On the one hand, it provides a mechanism whereby very short antigenic sequences spliced to the same host protein may result in cross-recognition of substantially different foreign antigens, however, we expect this to be unlikely due to the massive number of possible spliced peptides between the antigen and entire host proteome.

Overall, we believe that our framework provides a potential solution for efficacious gene therapy, not solely for Cas9-mediated genome engineering, but also for other protein therapeutics that might necessitate repetitive treatments. Although using this approach still requires mitigating the primary immune response, particularly antibody neutralization and CTL clearance, we expect that epitope deletion and low-immunogenicity delivery vectors such as AAVs will mitigate this problem, and the potential for repeated dosage will reduce the need for very high first-dose titers and efficiency.

METHODS

Computational Methods

k-mer Analyses—For Cas9, we initially chose 91 orthologs cited in exploratory studies cataloging the diversity of the Cas9 protein^{36,40,84–87}, including several that are experimentally well-characterized. We subsequently expanded our analysis to a total of 240 Cas9 orthologs and 44 Cpf1/Cas12a orthologs for DNA-targeting CRISPR-associated effector proteins, and 84 RNA-targeting CRISPR-associated effectors including Cas13a, b and c. For AAVs, we analyzed 167 sequences, focusing in on all 13 characterized human serotypes, as well as one isolate from rhesus macaque (rh32), one engineered variant (DJ), and one reconstructed ancestral protein (Anc80L65). We then compared total sequence similarity (immunologically uninformed) as well as predicted binding to class I and class II MHC molecules (immunologically informed) between these proteins. Immunologically uninformed sequence comparison was carried out by checking a sliding window of all contiguous k-mers in a protein for their presence in another protein sequence with either zero or one mismatch.

MHC Binding Predictions—Immunologically informed comparison was done in a similar fashion, but using only those k-mers predicted to bind to at least one of 81 HLA-1 alleles using netMHC 4.0⁸⁸ for class I (alleles can be found at http://www.cbs.dtu.dk/services/NetMHC/MHC_allele_names.txt), and at least one of 5,620 possible MHC II molecules based on 936 HLA-2 alleles using netMHCIIpan 3.1⁸⁹ for class II (alleles can be found at http://www.cbs.dtu.dk/services/NetMHCIIpan-3.1/alleles_name.list). We compared the use of netMHC to alternative immune epitope prediction platforms methods such as the

Immune Epitope Database (iedb.org)⁹⁰ and found very strong agreement across software. Ultimately, we chose netMHC because of the larger number of HLA alleles it supports. Sequences were defined as binding if the predicted affinity ranked in the top 2% of a test library of 400,000 random peptides as suggested in the software guidelines. Generation of immune orthogonal cliques was carried out using the Bron-Kerbosch algorithm. Briefly, a graph was constructed with each ortholog as a vertex, where the edges are defined by the number of shared immunogenic peptides between the connecting vertices. Sets of proteins for which every pair in the set is immune orthogonal constitutes a clique.

Phylogenetics and Species Classification—For phylogenetic analyses, protein sequences were aligned using MUSCLE, and distance was calculated using the BLOSUM 62 matrix excluding indels. Phylogeny of AAV serotypes was created using neighbor-joining on major serotype sequences. Categorization of Cas9 orthologs into commensal, pathogenic, environmental, and extremophile species of origin was done by assessing the source of the sample sequence. Sequences isolated from species which had been observed in human-associated samples were classified as pathogenic if they had been reported to cause disease (this would include species which are normally commensal, but opportunistically pathogenic), and commensal otherwise. Sequences from species which are not known to be associated with the human microbiome were classified as environmental unless the species was uniquely isolated from extreme environments including but not limited to geothermal vents, deep anoxic groundwater, fossil fuel deposits, and polar ice.

Experimental Methods

Vector design and construction—Split-SpCas9 AAV vectors were constructed by sequential assembly of corresponding gene blocks (IDT) into a custom synthesized rAAV2 vector backbone^{91,92}. The first AAV contains a gRNA driven by a human RNA polymerase III promoter, U6, and a N-terminal Cas9 (NCas9) fused to an N-intein driven by a CMV promoter, as well as a polyadenylation (polyA) signal. The second AAV cassette contains a CMV driven C-terminal Cas9 (CCas9) fused to a C-intein as well as a polyA signal. gRNA sequences were inserted into NCas9 plasmids by cloning oligonucleotides (IDT) encoding spacers into AgeI cloning sites via Gibson assembly. pX601-AAV-CMV::NLS-SaCas9-NLS-3xHA-bGHpA;U6::BsaI-sgRNA was a gift from Feng Zhang (Addgene plasmid # 61591).

AAV Production—AAV2/8, AAV2/2, AAV2/5, AAV2/DJ virus particles were produced using HEK293T cells via the triple transfection method and purified via an iodixanol gradient⁹³. Confluency at transfection was between 80% and 90%. Media was replaced with pre-warmed media 2 hours before transfection. Each virus was produced in 5 × 15 cm plates, where each plate was transfected with 7.5 µg of pXR-capsid (pXR-8, pXR-2, pXR-5, pXR-DJ), 7.5 µg recombinant transfer vector, and 22.5 µg of pAd5 helper vector using PEI (1 µg/µl linear PEI in 1x DPBS pH 4.5, using HCl) at a PEI:DNA mass ratio of 4:1. The mixture was incubated for 10 minutes at RT and then applied dropwise onto the media. The virus was harvested after 72 hours and purified using an iodixanol density gradient ultracentrifugation method. The virus was then dialyzed with 1x PBS (pH 7.2) supplemented with 50 mM NaCl and 0.0001% of Pluronic F68 (Thermo Fisher) using 100kDA filters

(Millipore), to a final volume of ~1 ml and quantified by qPCR using primers specific to the ITR region, against a standard (ATCC VR-1616).

AAV-ITR-F: 5'-CGGCCTCAGTGAGCGA-3' and

AAV-ITR-R: 5'-GGAACCCCTAGTGATGGAGTT-3'.

Animal studies—All animal procedures were performed in accordance with protocols approved by the Institutional Animal Care and Use Committee (IACUC) of the University of California, San Diego. All mice were acquired from Jackson labs. AAV injections were done in adult male C57BL/6J or BALB/c mice (10 weeks) through retro-orbital injections using 1×10^{12} vg/mouse.

CFA immunizations—CFA immunizations were prepared by mixing CFA (Sigma-Aldrich) with 5 μ g Cas9 protein or PBS at a 1:1 ratio using two syringes connected by an elbow joint to create an even emulsion. 200 μ L of CFA emulsion was injected subcutaneously into the flanks of adult mice.

ELISA

PCSK9: Levels of serum PCSK9 were measured using the Mouse Proprotein Convertase 9/PCSK9 Quantikine ELISA kit (R&D Systems) according to manufacturer's guidelines. Briefly, serum samples were diluted 1:200 in Calibrator diluent and allowed to bind for 2 h onto microplate wells that were precoated with the capture antibody. Samples were then sequentially incubated with PCSK9 conjugate followed by the PCSK9 substrate solution with extensive intermittent washes between each step. The amount of PCSK9 in serum was estimated colorimetrically using a standard microplate reader (BioRad iMark).

Cas9 and AAV: Recombinant SpCas9 protein (PNA Bio, cat. no. CP01), or SaCas9 protein (ABM good, cat no. K144), was diluted in 1x coating buffer (Bethyl), and 0.5 μ g was used to coat each well of 96-well Nunc MaxiSorp Plates (ab210903) overnight at 4 °C. For AAV experiments, 10^9 vg of AAV-2, -5, -8 or -DJ in 1x coating buffer was used to coat each well of 96-well Nuc MaxiSorp Plates. Plates were washed three times for 5 min with 350 μ l of 1x Wash Buffer (Bethyl) and blocked with 300 μ l of 1x BSA Blocking Solution (Bethyl) for 2 h at RT. The wash procedure was repeated. Serum samples were added at 1:40 dilution, and plates were incubated for 5 h at 4 °C with shaking. Wells were washed three times for 5 min, and 100 μ l of HRP-labeled goat anti-mouse IgG1 (Bethyl; diluted 1:100,000 in 1% BSA Blocking Solution) was added to each well. After incubating for 1hr at RT, wells were washed four times for 5 min, and 100 μ l of TMB Substrate (Bethyl) was added to each well. Optical density (OD) at 450 nm was measured using a plate reader (BioRad iMark).

NGS quantification of editing—Genomic DNA was extracted from samples of mouse livers using a DNA extraction kit (Qiagen). A 200 bp region containing the target cut site of the PCSK9 gene was amplified by PCR using 0.5 μ g DNA (~100,000 diploid genomes) as the template. Libraries were prepared using NEBNext Illumina library preparation kit and sequenced on an Illumina HiSeq. Each sample was sequenced to a target depth of 100,000

reads. Adaptors were trimmed from resulting fastqs using AdapterRemoval⁹⁴ and NHEJ-repaired cleavage events resulting in a mutation were quantified using CRISPResso⁹⁵.

Splenocyte Clearance Assay—Splenocyte clearance assays were performed similarly to previous work⁹⁶. Briefly, spleens from adult C57BL/6J mice were harvested and treated to remove erythrocytes and dead cells. These cells were then diluted to 10^7 cells/ml and split into two pools, one of which was pulsed for 40 min with a pool of the 30 most immunogenic T-cell epitopes in SpCas9 (according to our predictions) at $1 \mu\text{g/ml}$ each and labeled with the CellTrace Violet fluorescent dye (ThermoFisher). The other pool was pulsed with a matching amount of DMSO, and labeled with the green fluorescent dye CFSE (ThermoFisher). A 1:1 mixture of these cells were then injected into naïve or CFA-immunized mice at week 1 or 3.5 retro-orbitally at $3\text{--}6 \times 10^7$ cells per mouse. Spleens from these mice were harvested 16–20 hours later, treated to remove erythrocytes, and analyzed by flow cytometry to assess the degree of specific clearance of the CTV+ cells which were pulsed with Cas9 peptides.

Statistics—PCSK9 ELISA data from immunization experiments (Figures 3, S7), were normalized per mouse to the average of the first 4 weeks of the experiment (during which time no active dose was given), and then analyzed using a two-way repeated measures ANOVA to account for both time and group membership as independent variables. *Post hoc* Tukey tests were used to compare across groups at each timepoint as shown in Figure 3C.

Epitope prediction and peptide synthesis—The MHC-binding peptides for our mouse model were predicted using the netMHC-4.0 and netMHCIIpan-3.1 online software with the alleles H-2-Db and H-2-Kb for class I and H-2-IAb for class II. For MHCII, the top 10 peptides for Sp- and SaCas9 and top 5 peptides for AAV-8 and AAV-DJ by percentile binding were selected for synthesis by Synthetic Biomolecules as crude materials. For MHCI, we selected the top 20 peptides for Sp- and SaCas9 and the top 10 for AAV-8 and AAV-DJ. All peptides were dissolved in DMSO with a concentration of 40 mg ml^{-1} and stored at $-20 \text{ }^\circ\text{C}$.

IFN- γ ELISPOT assay—CD8+ T cells were isolated from splenocytes using magnetic bead positive selection (Miltenyi Biotec) 6 weeks after virus infection. A total of 2×10^5 CD8+ T cells were stimulated with 1×10^5 LPS-blasts loaded with $10 \mu\text{g}$ of individual peptide in 96-well flat-bottom plates (Immobilon-P, Millipore) that were coated with anti-IFN- γ mAb (clone AN18, Mabtech) in triplicate. Concanavalin A (ConA) was used as positive control. After 20 h of incubation, biotinylated anti-mouse IFN- γ mAb (R4-6A2; Mabtech), followed by ABC peroxidase (Vector Laboratories) and then 3-amino-9-ethylcarbazole (Sigma-Aldrich) were added into the wells. Responses are expressed as number of IFN- γ SFCs per 1×10^6 CD8+ T cells.

Supplementary Material

Refer to Web version on PubMed Central for supplementary material.

ACKNOWLEDGEMENTS

We thank members of the Mali lab for advice and help with experiments, and the Salk GT3 viral core for help with AAV production. This work was supported by UCSD Institutional Funds, the Burroughs Wellcome Fund (1013926), the March of Dimes Foundation (5-FY15-450), the Kimmel Foundation (SKF-16-150), and NIH grants (R01HG009285, R01CA222826, R01GM123313, R01AI079031 and R01AI106005). A.M. acknowledges a graduate fellowship from CONACYT and UCMEXUS.

REFERENCES

1. Mingozzi F & High KA Immune responses to AAV vectors: overcoming barriers to successful gene therapy. *Blood* 122, 23–36 (2013). [PubMed: 23596044]
2. Zaldumbide A & Hoeben RC How not to be seen: Immune-evasion strategies in gene therapy. *Gene Therapy* 15, 239–246 (2008). [PubMed: 18046427]
3. Yang Y, Li Q, Ertl HC & Wilson JM Cellular and humoral immune responses to viral antigens create barriers to lung-directed gene therapy with recombinant adenoviruses. *J. Virol* 69, 2004–15 (1995). [PubMed: 7884845]
4. Jawa V et al. T-cell dependent immunogenicity of protein therapeutics: Preclinical assessment and mitigation. *Clinical Immunology* 149, 534–555 (2013). [PubMed: 24263283]
5. Mays LE & Wilson JM The Complex and Evolving Story of T cell Activation to AAV Vector-encoded Transgene Products. *Mol. Ther* 19, 16–27 (2011). [PubMed: 21119617]
6. Basner-Tschakarjan E, Bijjiga E & Martino AT Pre-clinical assessment of immune responses to adeno-associated virus (AAV) vectors. *Frontiers in Immunology* 5, (2014).
7. Ertl HCJ & High KA Impact of AAV Capsid-Specific T-Cell Responses on Design and Outcome of Clinical Gene Transfer Trials with Recombinant Adeno-Associated Viral Vectors: An Evolving Controversy. *Hum. Gene Ther* 28, 328–337 (2017). [PubMed: 28042943]
8. Kotterman MA, Chalberg TW & Schaffer DV Viral Vectors for Gene Therapy: Translational and Clinical Outlook. *Annu. Rev. Biomed. Eng* 17, 63–89 (2015). [PubMed: 26643018]
9. Mingozzi F & High KA Therapeutic in vivo gene transfer for genetic disease using AAV: progress and challenges. *Nat. Rev. Genet* 12, 341–355 (2011). [PubMed: 21499295]
10. Manno CS et al. Successful transduction of liver in hemophilia by AAV-Factor IX and limitations imposed by the host immune response. *Nat. Med* 12, 342–347 (2006). [PubMed: 16474400]
11. Chew WL Immunity to CRISPR Cas9 and Cas12a therapeutics. *Wiley Interdiscip. Rev. Syst. Biol. Med* 10, e1408 (2018).
12. Sathish JG et al. Challenges and approaches for the development of safer immunomodulatory biologics. *Nat Rev Drug Discov* 12, 306–324 (2013). [PubMed: 23535934]
13. Harding FA, Stickler MM, Razo J & DuBridge RB The immunogenicity of humanized and fully human antibodies: Residual immunogenicity resides in the CDR regions. *MAbs* 2, 256–265 (2010). [PubMed: 20400861]
14. De Groot a S., Knopp PM & Martin W De-immunization of therapeutic proteins by T-cell epitope modification. *Dev. Biol. (Basel)* 122, 171–194 (2005). [PubMed: 16375261]
15. Tangri S et al. Rationally Engineered Therapeutic Proteins with Reduced Immunogenicity. *J. Immunol* 174, 3187 LP–3196 (2005). [PubMed: 15749848]
16. Ferdosi SR et al. Multifunctional CRISPR/Cas9 with engineered immunosilenced human T cell epitopes. *bioRxiv* (2018).
17. Salvat RS, Choi Y, Bishop A, Bailey-Kellogg C & Griswold KE Protein deimmunization via structure-based design enables efficient epitope deletion at high mutational loads. *Biotechnol. Bioeng.* 112, 1306–1318 (2015). [PubMed: 25655032]
18. Armstrong JK et al. Antibody against poly(ethylene glycol) adversely affects PEG-asparaginase therapy in acute lymphoblastic leukemia patients. *Cancer* 110, 103–111 (2007). [PubMed: 17516438]
19. Ganson NJ, Kelly SJ, Scarlett E, Sundy JS & Hershfield MS Control of hyperuricemia in subjects with refractory gout, and induction of antibody against poly(ethylene glycol) (PEG), in a phase I

- trial of subcutaneous PEGylated urate oxidase. *Arthritis Res. Ther* 8, R12–R12 (2006). [PubMed: 16356199]
20. Veronese FM & Mero A The impact of PEGylation on biological therapies. *BioDrugs* 22, 315–329 (2008). [PubMed: 18778113]
 21. Jevševar S, Kunstelj M & Porekar VG PEGylation of therapeutic proteins. *Biotechnol. J* 5, 113–128 (2010). [PubMed: 20069580]
 22. Jacobs F, Gordts SC, Muthuramu I & De Geest B The liver as a target organ for gene therapy: state of the art, challenges, and future perspectives. *Pharmaceuticals (Basel)*. 5, 1372–92 (2012). [PubMed: 24281341]
 23. Kok CY et al. Adeno-associated Virus-mediated Rescue of Neonatal Lethality in Argininosuccinate Synthetase-deficient Mice. *Mol. Ther* 21, 1823–1831 (2013). [PubMed: 23817206]
 24. Courtenay-Luck NS, Epenetos AA & Moore R Development of primary and secondary immune responses to mouse monoclonal antibodies used in the diagnosis and therapy of malignant neoplasms. *Cancer Res.* 46, 6489–6493 (1986). [PubMed: 2430699]
 25. Jinek M et al. A Programmable Dual-RNA – Guided DNA Endonuclease in Adaptive Bacterial Immunity. *Science* 337, 816–822 (2012). [PubMed: 22745249]
 26. Mali P et al. RNA-guided human genome engineering via Cas9. *Science* 339, 823–6 (2013). [PubMed: 23287722]
 27. Moreno AM & Mali P Therapeutic genome engineering via CRISPR-Cas systems. *Wiley Interdisciplinary Reviews: Systems Biology and Medicine* 9, (2017).
 28. Gasiunas G, Barrangou R, Horvath P & Siksnys V Cas9-crRNA ribonucleoprotein complex mediates specific DNA cleavage for adaptive immunity in bacteria. *Proc. Natl. Acad. Sci.* 109, E2579–E2586 (2012). [PubMed: 22949671]
 29. Cong L et al. Multiplex genome engineering using CRISPR/Cas systems. *Science* 339, 819–23 (2013). [PubMed: 23287718]
 30. Ran FA et al. In vivo genome editing using *Staphylococcus aureus* Cas9. *Nature* 520, 186–190 (2015). [PubMed: 25830891]
 31. Jinek M et al. RNA-programmed genome editing in human cells. *Elife* 2013, (2013).
 32. Mali P, Esvelt KM & Church GM Cas9 as a versatile tool for engineering biology. *Nat. Methods* 10, 957–963 (2013). [PubMed: 24076990]
 33. Hsu PD, Lander ES & Zhang F Development and applications of CRISPR-Cas9 for genome engineering. *Cell* 157, 1262–1278 (2014). [PubMed: 24906146]
 34. Kelton WJ, Pesch T, Matile S & Reddy ST Surveying the Delivery Methods of CRISPR/Cas9 for ex vivo Mammalian Cell Engineering. *Chim. Int. J. Chem* 70, 439–442 (2016).
 35. Cho SW, Kim S, Kim J-SJM & Kim J-SJM Targeted genome engineering in human cells with the Cas9 RNA-guided endonuclease. *Nat. Biotechnol* 31, 230–2 (2013). [PubMed: 23360966]
 36. Koonin EV, Makarova KS & Zhang F Diversity, classification and evolution of CRISPR-Cas systems. *Current Opinion in Microbiology* 37, 67–78 (2017). [PubMed: 28605718]
 37. Makarova KS et al. An updated evolutionary classification of CRISPR–Cas systems. *Nat. Rev. Microbiol* 13, 722–736 (2015). [PubMed: 26411297]
 38. Chylinski K, Makarova KS, Charpentier E & Koonin EV Classification and evolution of type II CRISPR-Cas systems. *Nucleic Acids Research* 42, 6091–6105 (2014). [PubMed: 24728998]
 39. Shmakov S et al. Diversity and evolution of class 2 CRISPR–Cas systems. *Nat. Rev. Microbiol* 15, 169–182 (2017). [PubMed: 28111461]
 40. Crawley AB, Henriksen JR & Barrangou R CRISPRdisco: An Automated Pipeline for the Discovery and Analysis of CRISPR-Cas Systems. *Cris. J* 1, 171–181 (2018).
 41. Charlesworth CT et al. Identification of Pre-Existing Adaptive Immunity to Cas9 Proteins in Humans. doi:10.1101/243345
 42. Wagner DL et al. High prevalence of *Streptococcus pyogenes* Cas9-reactive T cells within the adult human population. *Nat. Med* 1 (2018). doi:10.1038/s41591-018-0204-6
 43. Simhadri VL et al. Prevalence of Pre-existing Antibodies to CRISPR-associated Nuclease Cas9 in the US Population. *Mol. Ther. Methods Clin. Dev* (2018). doi:10.1016/j.omtm.2018.06.006

44. Wagner J a et al. Safety and biological efficacy of an adeno-associated virus vector-cystic fibrosis transmembrane regulator (AAV-CFTR) in the cystic fibrosis maxillary sinus. *Laryngoscope* 109, 266–74 (1999). [PubMed: 10890777]
45. Song S et al. Sustained secretion of human alpha-1-antitrypsin from murine muscle transduced with adeno-associated virus vectors. *Proc. Natl. Acad. Sci. U. S. A* 95, 14384–8 (1998). [PubMed: 9826709]
46. Chirmule N et al. Humoral Immunity to Adeno-Associated Virus Type 2 Vectors following Administration to Murine and Nonhuman Primate Muscle. *J. Virol.* 74, 2420–2425 (2000). [PubMed: 10666273]
47. Fields P a et al. Risk and prevention of anti-factor IX formation in AAV-mediated gene transfer in the context of a large deletion of F9. *Mol. Ther* 4, 201–210 (2001). [PubMed: 11545610]
48. Herzog RW et al. Influence of vector dose on factor IX-specific T and B cell responses in muscle-directed gene therapy. *Hum. Gene Ther* 13, 1281–91 (2002). [PubMed: 12162811]
49. Lozier JN, Tayebi N & Zhang P Mapping of genes that control the antibody response to human factor IX in mice. *Blood* 105, 1029–1035 (2005). [PubMed: 15383460]
50. Zhang HG et al. Genetic analysis of the antibody response to AAV2 and factor IX. *Mol. Ther* 11, 866–874 (2005). [PubMed: 15922957]
51. Tam HH et al. Sustained antigen availability during germinal center initiation enhances antibody responses to vaccination. *Proc. Natl. Acad. Sci. U. S. A* 113, E6639–E6648 (2016). [PubMed: 27702895]
52. Chew WL et al. A multifunctional AAV–CRISPR–Cas9 and its host response. *Nat. Methods* 13, 868–874 (2016). [PubMed: 27595405]
53. Benveniste O et al. Prevalence of Serum IgG and Neutralizing Factors Against Adeno-Associated Virus (AAV) Types 1,2,5,6,8, and 9 in the Healthy Population: Implications for Gene Therapy Using AAV Vectors. *Hum. Gene Ther* 21, 704–712 (2010). [PubMed: 20095819]
54. Gao G-P et al. Novel adeno-associated viruses from rhesus monkeys as vectors for human gene therapy. *Proc. Natl. Acad. Sci* 99, 11854–11859 (2002). [PubMed: 12192090]
55. Jooss K, Yang Y, Fisher KJ & Wilson JM Transduction of Dendritic Cells by DNA Viral Vectors Directs the Immune Response to Transgene Products in Muscle Fibers. *J. Virol* 72, 4212–4223 (1998). [PubMed: 9557710]
56. Gernoux G et al. Early Interaction of Adeno-Associated Virus Serotype 8 Vector with the Host Immune System Following Intramuscular Delivery Results in Weak but Detectable Lymphocyte and Dendritic Cell Transduction. *Hum. Gene Ther* 26, 1–13 (2015). [PubMed: 25333770]
57. Zhu J, Huang X & Yang Y The TLR9-MyD88 pathway is critical for adaptive immune responses to adeno-associated virus gene therapy vectors in mice. *J. Clin. Invest.* 119, 2388–2398 (2009). [PubMed: 19587448]
58. Gernoux G, Wilson JM & Mueller C Regulatory and Exhausted T Cell Responses to AAV Capsid. *Hum. Gene Ther* 28, 338–349 (2017). [PubMed: 28323492]
59. Kurosaki T, Kometani K & Ise W Memory B cells. *Nat. Rev. Immunol* 15, 149–159 (2015). [PubMed: 25677494]
60. Zabel F et al. Distinct T helper cell dependence of memory B-cell proliferation versus plasma cell differentiation. *Immunology* 150, 329–342 (2017). [PubMed: 27861835]
61. Ding Q et al. Permanent Alteration of PCSK9 With In Vivo CRISPR-Cas9 Genome Editing. *Circ. Res* 115, 488–492 (2014). [PubMed: 24916110]
62. Zinn E et al. In Silico Reconstruction of the Viral Evolutionary Lineage Yields a Potent Gene Therapy Vector. *Cell Rep* 12, 1056–1068 (2017).
63. Calcedo R & Wilson JM AAV Natural Infection Induces Broad Cross-Neutralizing Antibody Responses to Multiple AAV Serotypes in Chimpanzees. *Hum. Gene Ther. Clin. Dev* 27, 79–82 (2016). [PubMed: 27314914]
64. Harbison CE et al. Examining the cross-reactivity and neutralization mechanisms of a panel of mabs against adeno-associated virus serotypes 1 and 5. *J. Gen. Virol* 93, (2012).
65. Majowicz A et al. Successful Repeated Hepatic Gene Delivery in Mice and Non-human Primates Achieved by Sequential Administration of AAV5^{ch} and AAV1. *Mol. Ther* 25, 1831–1842 (2017). [PubMed: 28596114]

66. McIntosh JH et al. Successful attenuation of humoral immunity to viral capsid and transgenic protein following AAV-mediated gene transfer with a non-depleting CD4 antibody and cyclosporine. *Gene Ther* 19, 78–85 (2012). [PubMed: 21716299]
67. Mingozzi F et al. Prevalence and pharmacological modulation of humoral immunity to AAV vectors in gene transfer to synovial tissue. *Gene Ther* 20, 417–424 (2013). [PubMed: 22786533]
68. Mingozzi F et al. Pharmacological Modulation of Humoral Immunity in a Nonhuman Primate Model of AAV Gene Transfer for Hemophilia B. *Mol. Ther* 20, 1410–1416 (2017).
69. Unzu C et al. Transient and intensive pharmacological immunosuppression fails to improve AAV-based liver gene transfer in non-human primates. *J. Transl. Med* 10, 122 (2012). [PubMed: 22704060]
70. Riechmann L, Clark M, Waldmann H & Winter G Reshaping human antibodies for therapy. *Nature* 332, 323–7 (1988). [PubMed: 3127726]
71. Amabile A et al. Inheritable Silencing of Endogenous Genes by Hit-and-Run Targeted Epigenetic Editing. *Cell* 167, 219–232.e14 (2016). [PubMed: 27662090]
72. Hinderer C et al. Severe toxicity in nonhuman primates and piglets following high-dose intravenous administration of an AAV vector expressing human SMN. *Hum. Gene Ther. hum.* 2018.015 (2018). doi:10.1089/hum.2018.015
73. Vollmers C, Sit RV, Weinstein JA, Dekker CL & Quake SR Genetic measurement of memory B-cell recall using antibody repertoire sequencing. *Proc. Natl. Acad. Sci* 110, 13463–13468 (2013). [PubMed: 23898164]
74. Adamopoulou E et al. Exploring the MHC-peptide matrix of central tolerance in the human thymus. *Nat. Commun* 4, 2039 (2013). [PubMed: 23783831]
75. Ruppert J et al. Prominent role of secondary anchor residues in peptide binding to HLA-A2.1 molecules. *Cell* 74, 929–937 (2017).
76. Zhang S-Q et al. Direct measurement of T cell receptor affinity and sequence from naïve antiviral T cells. *Sci. Transl. Med* 8, 341ra77 (2016).
77. Baker MP, Reynolds HM, Lumicisi B & Bryson CJ Immunogenicity of protein therapeutics: The key causes, consequences and challenges. *Self Nonself* 1, 314–322 (2010). [PubMed: 21487506]
78. EL-Manzalawy Y, Dobbs D & Honavar V Predicting linear B-cell epitopes using string kernels. *J. Mol. Recognit* 21, 243–255 (2008). [PubMed: 18496882]
79. Larsen JEP, Lund O & Nielsen M Improved method for predicting linear B-cell epitopes. *Immunome Res.* 2, 2 (2006). [PubMed: 16635264]
80. Sollner J et al. Analysis and prediction of protective continuous B-cell epitopes on pathogen proteins. *Immunome Res.* 4, 1 (2008). [PubMed: 18179690]
81. Dalkas GA & Rooman M SEPIa, a knowledge-driven algorithm for predicting conformational B-cell epitopes from the amino acid sequence. *BMC Bioinformatics* 18, 95 (2017). [PubMed: 28183272]
82. Sun P et al. Bioinformatics resources and tools for conformational B-cell epitope prediction. *Computational and Mathematical Methods in Medicine* 2013, (2013).
83. Liepe J et al. A large fraction of HLA class I ligands are proteasome-generated spliced peptides. *Science* (80-.). 354, (2016).
84. Fonfara I et al. Phylogeny of Cas9 determines functional exchangeability of dual-RNA and Cas9 among orthologous type II CRISPR-Cas systems. *Nucleic Acids Res.* 42, 2577–2590 (2014). [PubMed: 24270795]
85. Shmakov S et al. Diversity and evolution of class 2 CRISPR–Cas systems. *Nat. Rev. Microbiol* 15, 169–182 (2017). [PubMed: 28111461]
86. Burstein D et al. New CRISPR–Cas systems from uncultivated microbes. *Nature* 542, 237–241 (2016). [PubMed: 28005056]
87. Shmakov S et al. Discovery and Functional Characterization of Diverse Class 2 CRISPR-Cas Systems. *Mol. Cell* 60, 385–397 (2015). [PubMed: 26593719]
88. Andreatta M & Nielsen M Gapped sequence alignment using artificial neural networks: application to the MHC class I system. *Bioinformatics* 32, 511–517 (2015). [PubMed: 26515819]

89. Andreatta M et al. Accurate pan-specific prediction of peptide-MHC class II binding affinity with improved binding core identification. *Immunogenetics* 67, 641–650 (2015). [PubMed: 26416257]
90. Vita R et al. The immune epitope database (IEDB) 3.0. *Nucleic Acids Res.* 43, D405–12 (2015). [PubMed: 25300482]
91. Truong D-JJ et al. Development of an intein-mediated split-Cas9 system for gene therapy. *Nucleic Acids Res.* 43, 6450–6458 (2015). [PubMed: 26082496]
92. Moreno AM et al. In Situ Gene Therapy via AAV-CRISPR-Cas9-Mediated Targeted Gene Regulation. *Mol. Ther* 0, (2018).
93. Grieger JC, Choi VW & Samulski RJ Production and characterization of adeno-associated viral vectors. *Nat. Protoc* 1, 1412–1428 (2006). [PubMed: 17406430]
94. Schubert M, Lindgreen S & Orlando L AdapterRemoval v2: rapid adapter trimming, identification, and read merging. *BMC Res. Notes* 9, 88 (2016). [PubMed: 26868221]
95. Pinello L et al. Analyzing CRISPR genome-editing experiments with CRISPResso. *Nat. Biotechnol* 34, 695–697 (2016). [PubMed: 27404874]

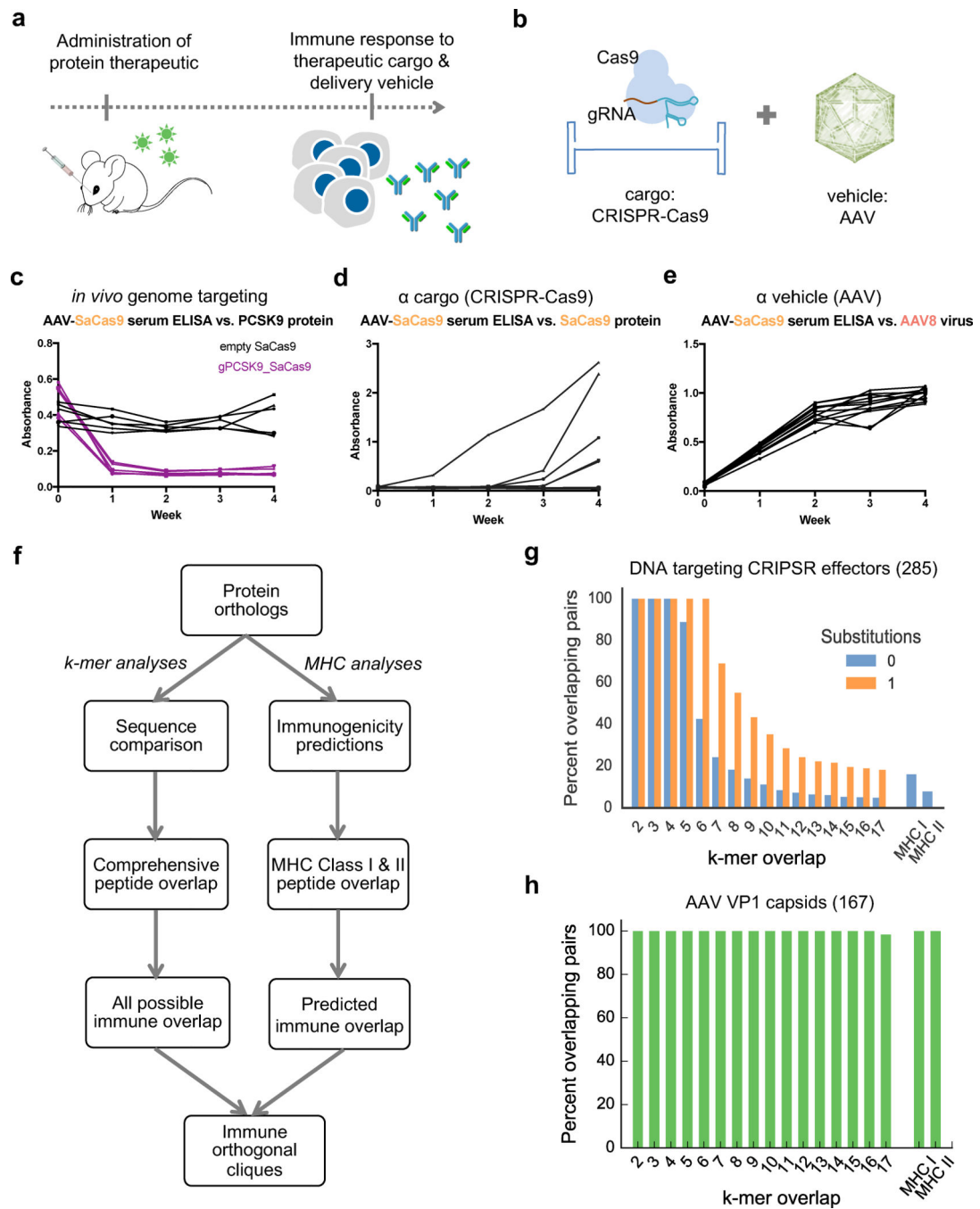


Figure 1: Protein based therapeutics elicit an adaptive immune response: experimental and *in silico* analyses.

(a) Proteins have substantial therapeutic potential, but a major drawback is the immune response to both the therapeutic protein and its delivery vehicle. (b) As a case study, we explored the CRISPR-Cas9 systems and corresponding delivery vehicles based on AAVs. (c) Mice were injected retro-orbitally with 10^{12} vg/mouse of AAV8-SaCas9 targeting the PCSK9 gene or a non-targeting control (empty vector). A decrease in PCSK9 serum levels, due to successful gene targeting, can be seen in mice receiving AAV-SaCas9-PCSK9 virus

(n=6 mice for each group). Each line represents an individual mouse. **(d)** Immune response to the payload was detected in ELISAs for the SaCas9 protein (n=12). Each line represents an individual mouse. **(e)** Immune response to the delivery vehicle was detected in ELISAs for the AAV8 virus capsid (n=12 mice). Each line represents an individual mouse. **(f)** *In silico* workflow used to find immune orthogonal protein homolog cliques. **(g)** Immunologically uninformed sequence comparison was carried out by checking all *k*-mers in a protein for their presence in another protein sequence with either zero or one mismatch. The x-axis corresponds to *k*, while MHC I and MHC II show overlap only of peptides predicted to bind to MHC class I and class II molecules. 48% of Cas9 pairs show no 6-mer overlap, and 79% of pairs show no overlapping MHC-binding peptides. **(h)** Same as (g) but for AAV VP1 capsid proteins. All AAV pairs contain overlapping MHC-binding peptides.

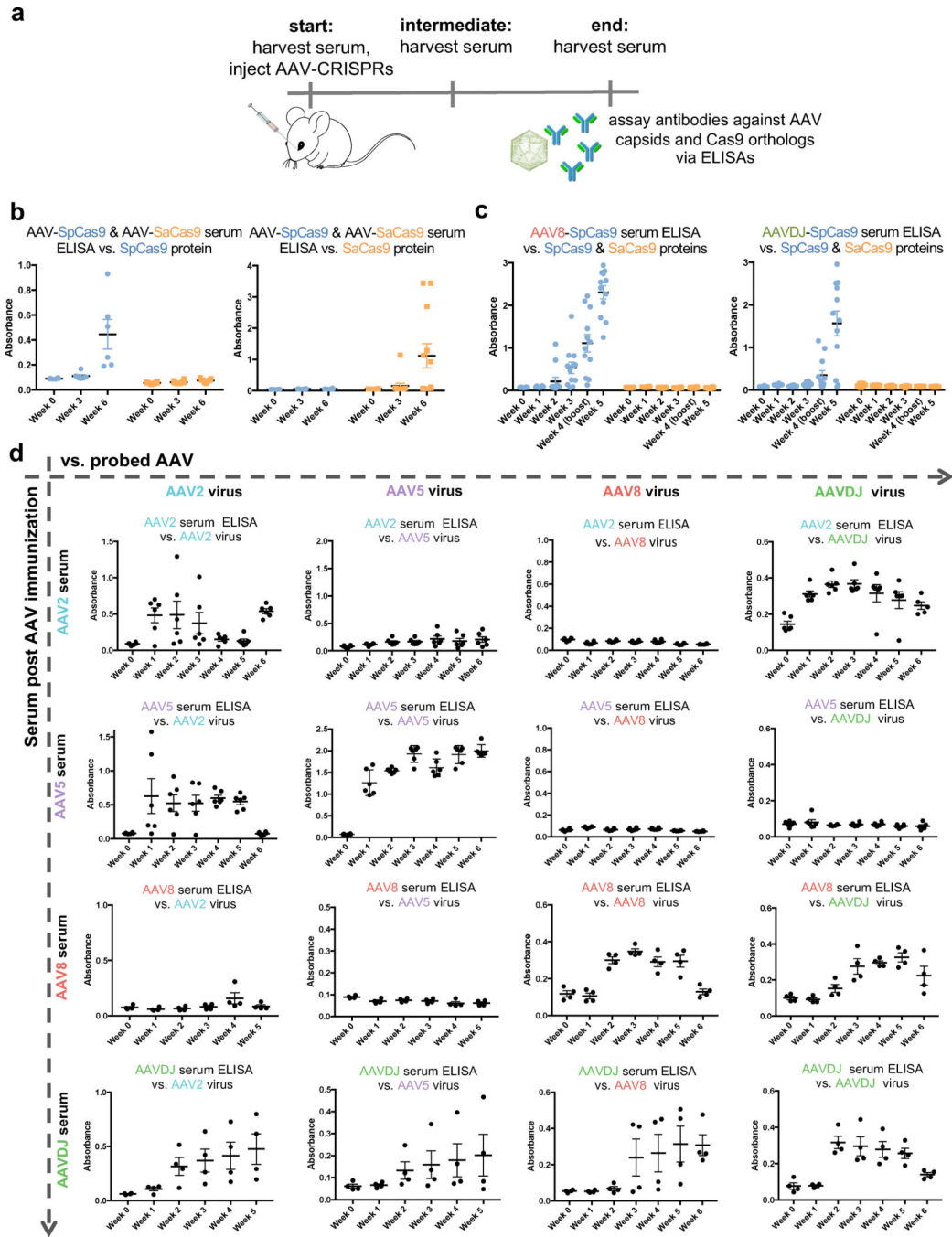


Figure 2: Experimental validation of Cas9 and AAV immunogenicity predictions.

(a) Mice were exposed to antigens via retro-orbital injections at 10^{12} vg/mouse. Serum was harvested prior to injection on day 0, and at multiple points over the course of 4–6 weeks. (b) anti-SpCas9 antibodies generated in mice injected with SpCas9 (n=6) and SaCas9 (n=12), and anti-SaCas9 antibodies generated in mice injected with SpCas9 (n=6) and SaCas9 (n=12). Results are shown as mean \pm s.e.m. Each data point represents an individual mouse. (c) anti-SpCas9 and anti-SaCas9 antibodies generated by mice injected with AAV8 SpCas9 (n=12; left panel), or AAVDJ SpCas9 (n=12; right panel). Results are shown as

mean \pm s.e.m. Each data point represents an individual mouse. **(d)** anti-AAV8/DJ/2/5 antibodies generated against mice injected with AAV8 or AAVDJ (n=4 for all panels), or with AAV2 or AAV5 (n=6 for all panels except for the AAVDJ serum ELISA at the week 6 time point where n=5). Results are shown as mean \pm s.e.m. Each data point represents an individual mouse.

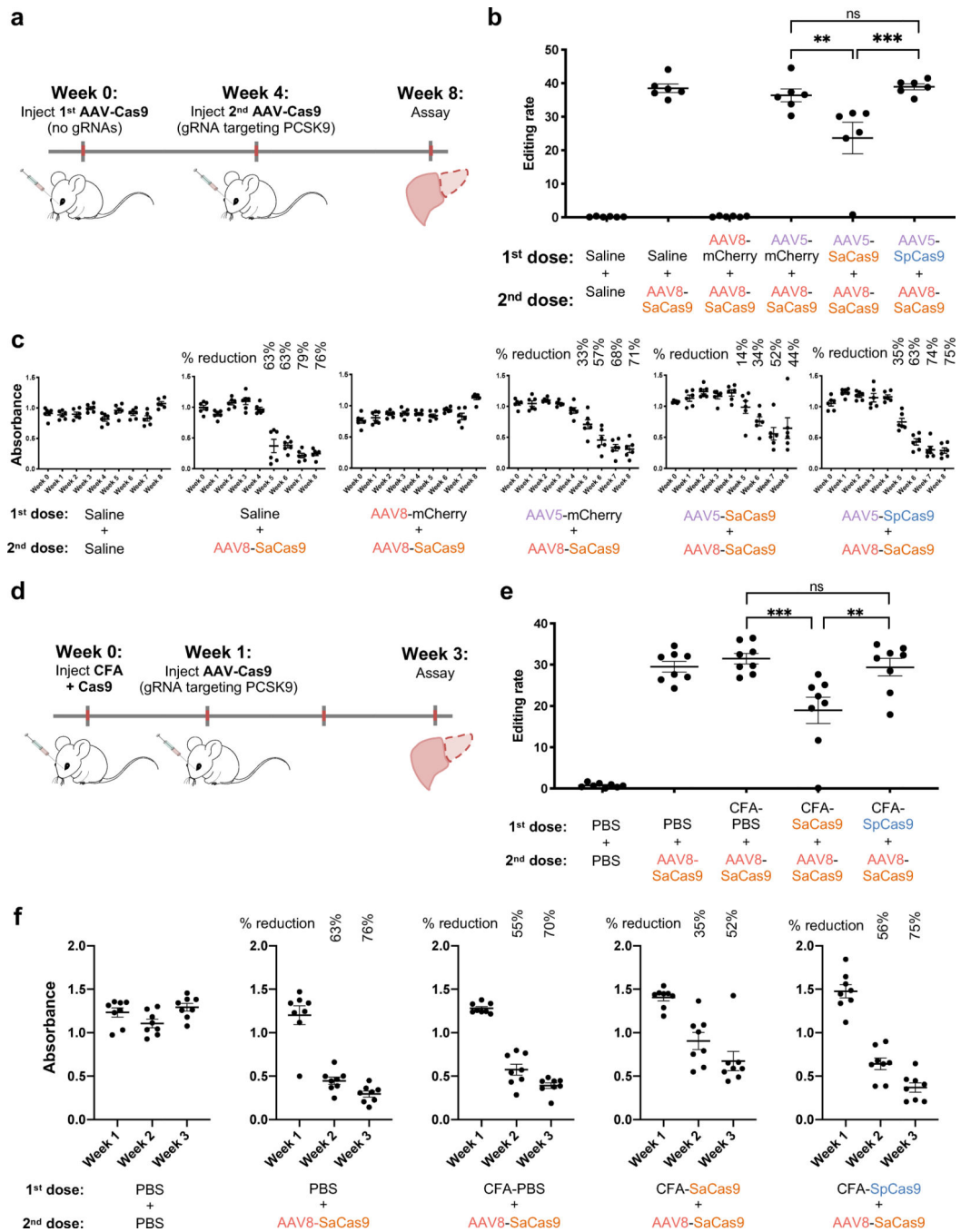


Figure 3: Engineering re-dosing with immune orthogonal orthologs.

(a) Mice were initially immunized with saline, AAV8-mCherry, AAV5-mCherry, AAV5-SaCas9, or AAV5-SpCas9 with no gRNA. After 4 weeks, the mice were given a second dose of saline or AAV8-SaCas9 with a gRNA targeting PCSK9. Serum was harvested prior to the first injection, and again at each subsequent week for 8 weeks. Mice were exposed to antigens via retro-orbital injections at 10^{12} vg/mouse. (b) Genome editing rates, quantified by sequencing, are entirely abolished when mice are immunized against AAV8, and moderately inhibited when immunized against SaCas9. No effect is seen when mice are

immunized against AAV5 or SpCas9. Results are shown as mean \pm s.e.m. A one-way ANOVA with *post hoc* Tukey's test was performed to determine statistical differences (**p=0.0033, ***p=0.0004, ns=not significant). Each data point represents an individual mouse (n=6 for all panels). (c) Final PCSK9 serum levels (week 8), the phenotypic result of gene editing, decrease sharply after an active second dose of AAV8-SaCas9 with gRNA. This effect is abolished when mice are first immunized against AAV8, but not when mice are first immunized against AAV5. Previous immunization with AAV5-SaCas9 reduces, but does not eliminate editing, whereas previous dosing with AAV5-SpCas9 has no effect on editing. Shown are the full time-course data for each week. Results are shown as mean \pm s.e.m. Each data point represents an individual mouse (n=6 for all panels). (d) Mice were immunized with CFA + 5 μ g Cas9 1 week prior to active AAV-SaCas9 injections. (e) At week 3, mice immunized with SaCas9 show a reduced editing rate compared to mice injected with CFA+PBS. No change in editing rate is seen when immunized with SpCas9. Results are shown as mean \pm s.e.m. A one-way ANOVA with *post hoc* Dunnett's test was performed to determine statistical differences (***p=0.0002, **p=0.0015, ns=not significant). Each data point represents an individual mouse (n=8). (f) Serum PCSK9 reduction is partially inhibited when mice are immunized with CFA+SaCas9, but not CFA+PBS or CFA+SpCas9. Results are shown as mean \pm s.e.m. Each data point represents an individual mouse (n=8).